Acta Crystallographica Section D
Biological Crystallography
ISSN 0907-4449

The influence of an internal electric field upon protein crystallization using the gel-acupuncture method

N. Mirkin, B. A. Frontana-Uribe, A. Rodríguez-Romero, A. Hernández-Santoyo and A. Moreno*

Instituto de Química, UNAM Circuito Exterior, C. U. Mexico, D. F. 04510, Mexico

Correspondence e-mail: carcamo@servidor.unam.mx

Received 9 September 2002
Accepted 11 June 2003

In this work, the influence of an internal electric field upon the crystallization of lysozyme and thaumatin is explored using a modified design of the gel-acupuncture setup. From a crystallographic point of view, the orientation of crystals that grow preferentially over different types of electrodes inside capillary tubes is also evaluated. Finally, the crystal quality and the three-dimensional structure of these proteins grown with and without the electric field influence are analyzed by means of X-ray diffraction methods.

1. Introduction

The major problem in producing suitable protein crystals for X-ray diffraction or biophysicochemical investigations lies in the limited amount of protein to be analyzed or crystallized. Nowadays, newer, more efficient and faster methods for protein overexpression using molecular biology have been proposed for high-throughput analyses in order to perform protein crystallization and consequently X-ray crystallographic investigations. However, there are some physicochemical parameters which could improve protein crystal growth or control nucleation phenomena that have not been fully explored. These parameters are the magnetic field (Sazaki *et al.*, 1997; Ataka *et al.*, 1997; Wakayama *et al.*, 1997; Yanagiya *et al.*, 2000), electrofocusing (McPherson, 1992) and the influence on the nucleation and crystal growth of biological macromolecules using an external electric field (Taleb *et al.*, 1999, 2001; Nanev & Penkova, 2001, 2002).

There are only a few recent studies in which the influence of an external electric field upon protein crystallization has been evaluated using the batch, hanging-drop and sitting-drop methods. For instance, using droplet techniques in the laboratory of Aubry and coworkers it has been proved that an external electric field suppresses HEWL crystal nucleation, resulting in an increased growth rate of lysozyme crystals in the external electric field (Taleb *et al.*, 1999). Most recently, Aubry and coworkers (Taleb *et al.*, 2001) measured the kinetics of the protein crystallization process and detected increased HEWL concentration in the solution near the cathode. On the other hand, in work published by Nanev & Penkova (2001) crystal growth was conducted using templates of organic polymers inside capillary tubes. Using the batch method, the effect on lysozyme crystallization of applying electric and ultrasonic fields was evaluated. It was also observed that the orientational growth of the crystals followed a preferential direction towards the cathode. Most recently, Nanev and coworkers have evaluated lysozyme crystals to be preferentially orientated along the *c* axis when a magnetic field is applied; the critical temperature at which the effect is

more remarkable has also been determined (Nanev & Penkova, 2002).

However, all of these publications lack crystallographic data or structural analyses for the crystals grown in the electric field. In none of them is there any indication of crystal-packing modifications. It may be useful to find a new experimental method that could be used to study the effects of electric fields upon protein crystallization and establish a theoretical basis that would explain what happens during crystal nucleation and growth.

In this work, we tried (i) to explore the influence of an internal electric field during the crystallization of lysozyme and thaumatin using a modified design of the gel-acupuncture setup (García-Ruiz *et al.*, 1993; García-Ruiz & Moreno, 1994) and (ii) to study the polarity effect of the electrodes and the current interval at which the internal electric field had the strongest influence on either the crystallization process or the nucleation phenomena. Finally, we also evaluated the crystal quality as well as the three-dimensional structure of the crystals grown in the presence or absence of the electric field.

2. Materials and methods

All these experiments were performed using an *ad hoc* modified Granada Crystallization Box (Hampton Research) commonly used for the gel-acupuncture method. In this new configuration, two electrodes and a direct current power supply (Galvanostat EG&G Princeton Applied Research, Model 173) were adapted as shown in Fig. 1. The applied current ranged from 0.9 to 1.0 μA so that the maximal current density was 2.86 μA cm^{-2} and was kept constant during the crystallization process. The electrodes used were platinum wires (0.2 mm diameter) and graphite rods (0.5 mm diameter). All experiments were carried out at constant temperature (291 ± 0.1 K), but it is worth mentioning that the temperature inside the capillary tube may be slightly different owing to the heat released by the applied current and ionic movement. A 100 mg ml^{-1} solution of lysozyme (Sigma L-6876) was prepared in 100 m*M* sodium acetate buffer pH 4.6 and 20%(*w*/*v*) NaCl in water (as the crystallizing agent). For thaumatin (Sigma T-7638), a 100 mg ml^{-1} solution in water and 25%(*w*/*v*) sodium potassium tartrate in 100 m*M* buffer phosphate pH 7.0 was used as the crystallization agent.

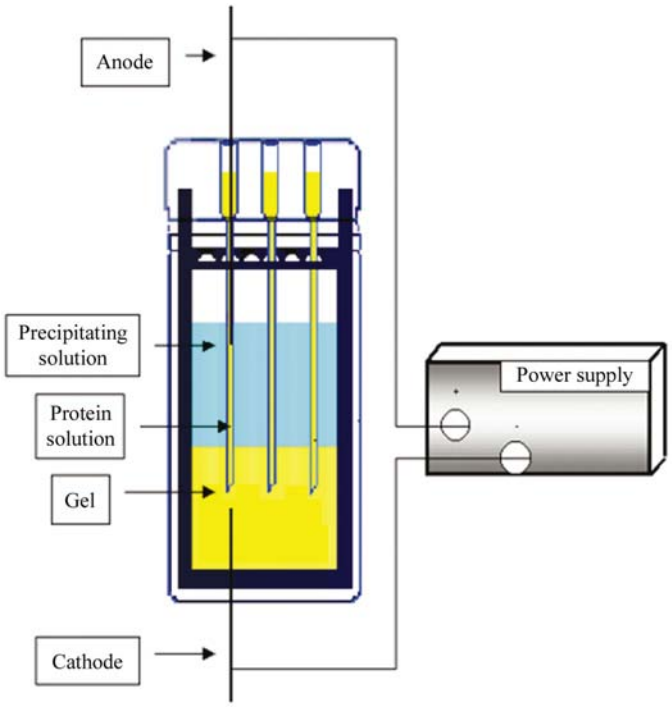

Figure 1
Experimental setup of the crystallization cell connected to a power supply (galvanostat).

The electrodes were introduced through two orifices in the crystallization cell. The capillary tube was first filled with protein solution and one electrode was placed inside, allowing the tip to protrude out of the capillary tube for connection to the power source. The upper part of the tube (where the electrode protrudes) was sealed with wax. The open-ended part of the capillary tube was punctured into the gel in the lower part of the crystallization cell; the other electrode was then introduced and the capillary tube sealed with the same sealant. In all the experiments carried out with the gel-acupuncture method, we kept the same penetration length of 5 mm. Once the crystallization agent was poured onto the gel, the system was connected to a direct-current power supply (galvanostat). For each experiment there was a corresponding control experiment in which the electrodes were dipped into the protein solution and the gel, but no current was applied. The protein solutions were in contact with the anode in most of the experiments used to test the influence of the internal electric field. By changing the polarity of the galvanostat, the effect of the cathode immersed into the protein solution was also examined. Initially, capillary tubes of 1.0 mm diameter were used. However, in the preliminary experiments some bubbles were formed owing to electrolysis of water. These bubbles block protein diffusion towards the electrode, interrupting the electric current. To overcome this problem, wider capillary tubes of 1.5 mm internal diameter were used. The effect of the electric field on the crystallization process was followed by taking optical images using a Zeiss Stemi SV11 stereoscopic microscope with a CCD camera adapted to our experimental setup. The program *AxioVision* provided by Zeiss Co. was used to record the digital images.

Once crystals were obtained on the electrode, at least four of them were removed, mounted in a clean capillary and X-ray data collection was performed at 291 K using a Rigaku R-AXIS IIc diffractometer with a rotating-anode generator (operated at 50 kV, 100 mA). Diffraction data were integrated using the *DENZO* program (Otwinowski & Minor, 1997) and scaled with programs from the *CCP*4 suite (Collaborative Computational Project, Number 4, 1994). The three-dimensional structure was obtained using the molecular-replacement method and data from the PDB for thaumatin (PDB code 1thw) where needed. Molecular-replacement and rigid-body refinement was accomplished using *CNS* v.1.0 (Brünger *et al.*, 1998), while model-building and correction

procedures were performed using the program *QUANTA*2000 (Molecular Simulations Inc., Burlington, MA, USA). *PROCHECK* (Laskowski *et al.*, 1993) was used for analysing the stereochemistry of the model.

3. Results and discussion

3.1. Observations of the general crystal-growth behavior

The crystallization conditions used were those typically used for lysozyme and thaumatin crystallization in the gel-acupuncture method (García-Ruiz *et al.*, 1993; García-Ruiz & Moreno, 1994). For lysozyme, a precipitate appeared within a few minutes in the lower part of the capillary tube when the electrodes were connected to the galvanostat. This behavior is usually observed using the typical gel-acupuncture method; nevertheless, when the electrical current was applied the precipitate and the crystals were obtained in a shorter time. The precipitate increased in height up to the electrode tip, covering the lower area of the electrode. On the other hand, when the electrodes were very close to one another, the precipitate moved along the electrode towards its upper part. Crystals were obtained in less than 24 h, keeping a homogenous morphology of the tetragonal system of lysozyme around the electrodes (Pt and graphite) compared with the control. In the case of thaumatin, this initial precipitate was not observed. The most remarkable result was the following: crystals of thaumatin are usually obtained in approximately 12 d using the common gel-acupuncture setup, whereas with the influence of electric current crystals were obtained in 5 d. It is worth mentioning that these crystals of thaumatin were larger than those observed for the control and the apparent mosaicity was not very different, as will be shown in §3.3.

These effects on the crystal-growth behavior led us to establish that the influence of the fields could effect (i) the kinetics of the process (related to the nucleation and the mechanisms of crystal growth) and (ii) changes in the three-dimensional crystal structure. Concerning the first point, we evaluated the growth rate *versus* time for one of the studied proteins. Fig. 2 shows the average growth rate of lysozyme crystals grown under the influence of an electric current compared with the control. The plot shows that the crystals grown under the influence of a direct current grew faster than those grown using the classical experimental setup without current.

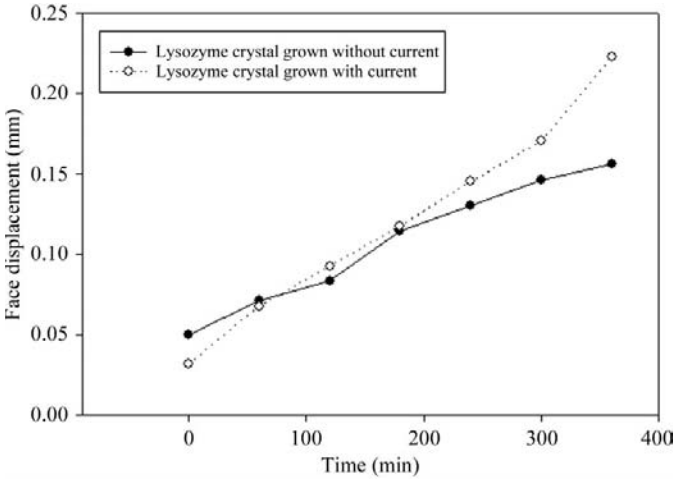

Figure 2
Plot of the average growth rate for two crystals of lysozyme: (*a*) control, (*b*) crystal grown under the influence of an electric field.

In relation to the preferential orientation of the crystals, we observed that for all crystals attached to the electrode there seem to be preferential faces that used the electrode as a substrate in the presence of the electric field. These faces were mostly oriented towards the *c* axis of the tetragonal crystal of lysozyme. It is very important to mention that in all cases crystals appeared on the anode. When the polarity of the electrodes was changed (with the working electrode now behaving as a cathode), we did not observe the same crystal-growth behavior. We only obtained aggregates deposited on the surface of the electrode and most of the time amorphous precipitation was observed during the crystallization experiment. Because of these results, other variables, such as the material of the electrode, the strength of the electric field or the charge density over the electrode, needed to be evaluated.

In order to understand the nucleation behavior of the protein molecule inside the capillary tube with a dipped electrode (anode), the existence of an electric double layer formed along the electrode must be considered. It is well known that when an electrode is dipped into an electrolyte solution, an electric double layer is formed around the metal owing to the asymmetric forces felt by the electrolytes.

This double layer is composed of an initial plane of water molecules with their dipoles oriented with respect to the electrode charge. There is also a second plane in which hydrated ions of opposite charge arrange around it (Bard & Faulkner, 2001). The anomalous behavior of the attachment of lysozyme (positively charged at the pH value of the buffer) to the anode (a positively charged electrode dipped in the capillary tube containing the protein solution) may arise from the interaction of lysozyme with the ions present in the electric double layer around the electrode. In Fig. 1, a reversal of the polarity of the electrodes, in which the electrode in the capillary tube is working as the cathode, is represented. This experimental setup produces a migration of the negatively charged ions towards the anode (immersed in the gel). Therefore, the capillary tube will be mainly filled with the positively charged ions (Na^+) as well as the protein molecule itself (positively charged at this pH value). This effect leads to a disturbance of the system owing to the fact that negatively charged ions (Cl^-) are needed for the protein–protein interactions in lysozyme crystallization (Vaney *et al.*, 2001). This overview explains why the crystals grew on the surface of and around the electrode when it was used as an anode. This electrochemistry-based method of crystallizing proteins is not an electrocrystallization because there is no redox reaction occurring between the protein and the electrode, but there is an electro-focusing or electro-dialysis arising from the applied current. Something similar to this occurs in the classical electrophoresis method.

The crystals of lysozyme grew on the surface and around the anode (dipped in the capillary tube containing protein solution) instead of appearing on the cathode part. The same crystal-growth behavior was observed when thaumatin was crystallized. However, in this case the crystallization conditions were different (precipitating agent, pH of buffer solution), although the crystal-growth trend was the same as that observed for lysozyme. It is worth mentioning that thaumatin and lysozyme were prepared in different buffer solutions (pH 7 and pH 4.5, respectively). However, both proteins were positively charged in solution owing to the similar values of their isoelectric points (11.4 for lysozyme and 12 for thaumatin).

3.2. The influence of the distance and materials of the electrodes and the pH variation during the crystallization process

In order to attempt to explain the attachment of crystals to the positively charged electrode, the effect of the use of two different materials, platinum and graphite, as electrodes was examined. In order to perform this, the anode was dipped into the lysozyme solution and the cathode was immersed in the gel part. By using the graphite electrode, several crystals were obtained in the solution and a very few small well shaped protein crystals were observed adsorbed on the electrode. On the other hand, for the Pt-wire electrode the crystals were of a larger size and showed regular tetragonal morphology. Some of them were adsorbed and some were located around the electrode after 24 h (Fig. 3). Additionally, the pH variation in our experimental setup was examined using acid–base indicators. In addition to water electrolysis, it was also necessary to confirm that the pH value did not change around the electrode. We observed neither considerable variations of the pH value nor water electrolysis when low values of direct current were applied.

After finding the most appropriate electrode, platinum wire, the influence of the strength of the electric field was studied by changing the distances between the electrodes. For a constant electric current (using this experimental setup), it was established that the more we separated the electrodes, the weaker the electric field. When the distance between the electrodes was changed, it was observed that the more they were separated, the more typical were both the morphology of the obtained lysozyme crystals compared with the control experiment and the induction time for the nucleation. When the distance between the electrodes was reduced, lysozyme crystals were obtained in a shorter time. The same effect of the distance between electrodes was observed for thaumatin: the larger the distances, the smaller the difference from the control experiment.

Table 1
X-ray data statistics for the thaumatin crystals.

	Control	Electhau1	Electhau2
Data collection			
Space group	$P4_12_12$	$P4_12_12$	$P4_12_12$
Unit-cell parameters (Å)			
a	58.664	58.647	58.633
b	58.664	58.647	58.6337
c	151.391	151.390	151.427
Resolution range (Å)	15.0–2.0	15.0–2.0	15.0–2.0
No. of reflections	135685	134546	105150
No. of unique reflections	18694	19702	19204
$I/\sigma(I)$	9.0	3.6	7.8
Completeness	99.2	98.8	96.5
R_{merge} (%)	0.053	0.112	0.059
Structure refinement			
R/R_{free}	0.177/0.205	0.192/0.224	0.173/0.187
Average *B* factor	23.4	24.2	22.6
R.m.s. deviations			
Bonds (Å)	0.005	0.005	0.005
Angles (°)	1.3	1.3	1.3
Torsions (°)	25.3	25.2	25.4
No. of non-H atoms			
Protein	1545	1546	1548
Ligand	10	10	10
Water	93	97	98

3.3. The analysis of the crystal quality and three-dimensional structure of thaumatin by means of X-ray diffraction methods

In order to obtain some idea of the changes in the three-dimensional structure when a direct current was applied, one of the model proteins where better X-ray data were found in our experimental X-ray measurements was chosen. A comparison was made between thaumatin crystals grown with and without the electric field. X-ray diffraction methods were used to analyze and compare the thaumatin crystal symmetry. All analyzed crystals showed the same tetragonal morphology and belonged to space group $P4_12_12$. The X-ray data statistics are shown in Table 1. From this table, the statistics for the

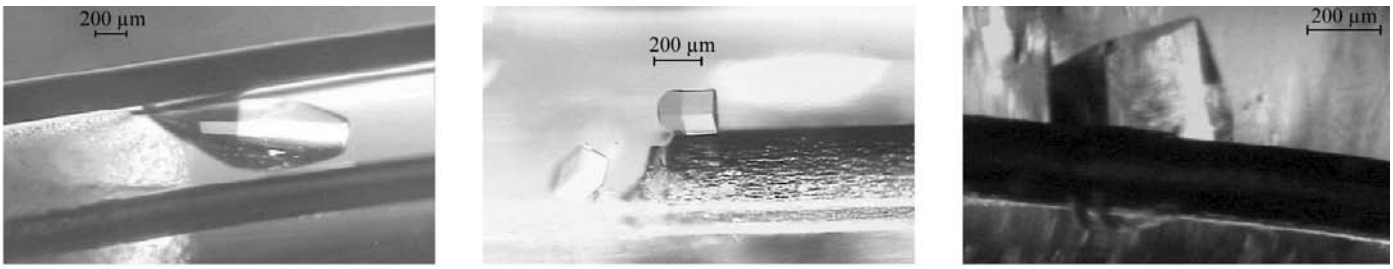

Figure 3
Lysozyme crystals grew attached to the electrode (Pt and graphite), while many others were obtained in the solution: (*a*) control, (*b*) when graphite anode was used, (*c*) a general view when a Pt anode was used.

crystals named electhau1 and electhau2 correspond to two crystals grown inside the capillary tube where the electrodes were separated by 2 cm. The crystals seemed to be packed in the same way independently of the applied electric current. It was also necessary to evaluate the crystal quality by using a plot of $I/\sigma(I)$ (intensity/estimated error) *versus* R (resolution) for each protein in order to compare them with the control. Fig. 4 shows this result for thaumatin crystals grown under the influence of an internal electric field. The other crystal was grown with dipped electrodes but without applying current (control). This plot of $I/\sigma(I)$ showed that the crystal grown in the electric field is significantly more disordered than that in the control. The increased lattice disorder associated with rapid crystal growth led to the two plots in Fig. 4. As is observed in this plot, the crystal quality (in terms of the randomness in the crystal) was slightly modified owing to the influence of the electric current. However, when the apparent mosaicity for both cases was analyzed, there was no significant difference, *i.e.* 0.20 for the control thaumatin crystal and 0.24 for the crystal of thaumatin grown in the electric field. This increased lattice disorder associated with rapid crystal growth represents an apparent disadvantage in terms of structural packing when a current is applied. Nevertheless, we have to consider that if there are no changes in the three-dimensional structure, the advantage of this method will be the shorter induction time for the nucleation phenomena and the crystal-growth stage.

In order to characterize any structural changes that occur when applying the direct current during the crystallization process of thaumatin and lysozyme, it was necessary to solve the three-dimensional structure of those protein crystals by the molecular-replacement method. From the X-ray data collection, we obtained higher quality data sets for thaumatin crystals, so that we decided to focus our structural analyses on this model protein in order to analyze the three-dimensional protein structure.

We compared the structure of two protein crystals of thaumatin, one grown under the influence of an electric current and the other without any electric influence. No structural differences in the polypeptide chain were observed. Comparison of the Ramachandran plots of a crystal grown under the influence of an electric field, a control crystal and data taken from the PDB (PDB code 1thw) was performed. From these plots, there was only one missing residue in the three cases, which was located in the forbidden area of the Ramachandran plot. This electron density was observed after solving and refining the three-dimensional structure for all the analyzed protein crystals (control crystal and crystals grown under the electric influence). This electron density corresponded to Asp25, which was observed in all cases to be inside the electron-density map of the polypeptide chain without any anomalous electron-density distribution along the chain. This aspartate residue was located in the loop insertion between β-strands B and C as reported by Ko *et al.* (1994). This deviation of the main-chain–main-chain dihedrals might be indicative of the functionally important regions of a protein (Asp25), as pointed out by Unger & Moult (1993).

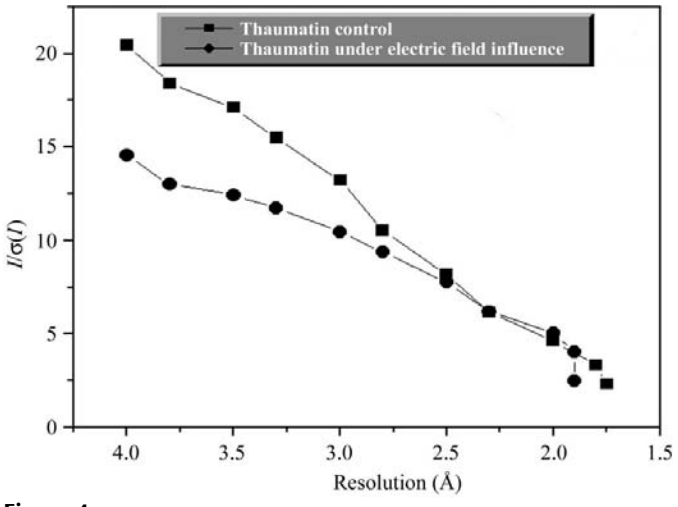

Figure 4
Plot of $I/\sigma(I)$ *versus* R for testing the crystal packing of thaumatin grown with and without the influence of the internal electric field.

Based on our results, we suggest that one of the main advantages of this method of crystal growth is the shorter time required to obtain crystals compared with the typical experimental setup of the gel-acupuncture method. On the other hand, the three-dimensional structure is not affected by the current applied during the crystal-growth process, as was shown by the X-ray crystallographic analyses. Because the applied current is small, the effect is not enough to change the space group of the crystal, although it did lead to more randomness in it, slightly modifying the protein crystal quality. The most remarkable observation compared with the lysozyme and thaumatin controls was the shorter time required for the nucleation and crystal-growth stages. In order to investigate any biochemical changes in the protein structure when the electric field was applied, we collected several crystals grown under the influence of an internal electric field and compared them with the control experiments using the gel-electrophoresis method. The electrophoresis gel showed the same bands as for the controls. For the crystals (lysozyme and thaumatin) obtained under the influence of an internal electric field, there was no substantial difference between the crystals dissolved in solution. Therefore, the crystal-packing quality is only different in the solid state when the current is applied and when the nuclei are formed, but the crystal maintains its structure and symmetry (as seen from the X-ray data).

4. Conclusions

This work was a preliminary approach focused on the description of the *ad hoc* modified Granada crystallization cell using the gel-acupuncture setup to investigate the influence of an internal electric field during the crystallization process. Very interesting results concerning the induction time for the nucleation were observed as a result of the presence of this internal electric current along the capillary tube. This information will not only reopen a new area of research on the internal influences of the electric field on protein crystallization, but it will also provide new insights into the solubility

behavior of proteins, with relevance to understanding the nucleation and the crystallization process, and controlling the size of the crystals. As was shown in the X-ray diffraction experiments, the same space groups were obtained for lysozyme and thaumatin crystals after applying the internal electric field, without affecting the three-dimensional structure, even though the solubility was modified in some way (as observed by the lower number of crystals obtained). Further studies will be focused on explaining whether the decrease in the induction time for nucleation arising from the internal electric field can only be observed in these proteins or whether it is a common effect for all proteins. From the three-dimensional structure data of these analyzed crystals, it can be said that the structure of the protein is not modified but that it is possible to control either the induction time for the nucleation or the direction of the crystallization on the surfaces of the electrodes depending of their polarity.

Authors acknowledge grants from CONACYT-México projects 36155E, J34873-E, 3241E and DGAPA-UNAM project No. IN204702. This is publication number 1766 from the Instituto de Química, UNAM, México. NM acknowledges a doctoral scholarship from DGEP-UNAM and the authors are indebted to Miss Gabriela Salcedo for language correction.

References

Ataka, M., Katoh, E. & Wakayama, N. I. (1997). *J. Cryst. Growth*, **173**, 592–596.

Bard, A. J. & Faulkner, L. R. (2001). *Electrochemical Methods, Fundamentals and Applications*. New York: Wiley & Sons.

Brünger, A. T., Adams, P. D., Clore, G. M., DeLano, W. L., Gros, P., Grosse-Kunstleve, R. W., Jiang, J. S., Kuszewski, J., Nilges, M., Pannu, N. S., Read, R. J., Rice, L. M., Simonson, T. & Warren, G. L. (1998). *Acta Cryst.* D**54**, 905–921.

Collaborative Computational Project, Number 4 (1994). *Acta Cryst.* D**50**, 760–763.

García-Ruiz, J. M. & Moreno, A. (1994). *Acta Cryst.* D**50**, 484–490.

García-Ruiz, J. M., Moreno, A., Viedma, C. & Coll, M. (1993). *Mater. Res. Bull.* **232**, 285–293.

Ko, T.-P., Day, J., Greenwood, A. & McPherson, A. (1994). *Acta Cryst.* D**50**, 813–825.

Laskowski, R. A., MacArthur, M. W., Moss, D. S. & Thornton, J. M. (1993). *J. Appl. Cryst.* **26**, 283–291.

McPherson, A. (1992). *J. Cryst. Growth*, **122**, 161–167.

Nanev, Ch. & Penkova, A. (2001). *J. Cryst. Growth*, **232**, 285–293.

Nanev, Ch. & Penkova, A. (2002). PhD thesis, Bulgarian Academy of Sciences, Bulgaria.

Otwinowski, Z. & Minor, W. (1997). *Methods Enzymol.* **276**, 307–326.

Sazaki, G., Yoshida, E., Komatsu, H., Nakada, T., Miyashita, S. & Watanabe, K. (1997). *J. Cryst. Growth*, **173**, 231–234.

Taleb, M., Didierjean, C., Jelsch, C., Mangeot, J. P. & Aubry, A. (2001). *J. Cryst. Growth*, **232**, 250–255.

Taleb, M., Didierjean, C., Jelsch, C., Mangeot, J. P., Capelle, B. & Aubry, A. (1999). *J. Cryst. Growth*, **200**, 575–582.

Vaney, M. C., Broutin, I., Retailleau, P., Douangmath, A., Lafont, S., Hamiaux, C., Prangé, T., Ducruix, A. & Riès-Kautt, M. (2001). *Acta Cryst.* D**57**, 929–940.

Unger, R. & Moult, J. (1993). *Bull. Math. Biol.* **55**, 1183–1198.

Wakayama, N. I., Ataka, M. & Abe, H. (1997). *J. Cryst. Growth*, **178**, 653–656.

Yanagiya, S., Sazaki, G., Miyashita, S., Nakajima, K., Komatsu, H., Watanabe, K. & Motokawa, M. (2000). *J. Cryst. Growth*, **208**, 645–650.